

UC Irvine

UC Irvine Electronic Theses and Dissertations

Title

Photothermal Heating of Nanoparticles for Radical Polymerization

Permalink

<https://escholarship.org/uc/item/2q69s47f>

Author

Steeves, Timothy McCormick

Publication Date

2017

Peer reviewed|Thesis/dissertation

UNIVERSITY OF CALIFORNIA,
IRVINE

Photothermal Heating of Nanoparticles for Radical Polymerization

THESIS

submitted in partial satisfaction of the requirements
for the degree of

MASTER OF SCIENCE

in Chemistry

by

Timothy McCormick Steeves

Thesis Committee:
Associate Professor Aaron Esser-Kahn, Chair
Assistant Professor Shane Ardo
Professor Zuzanna Siwy

2017

DEDICATION

To my parents and sister,
whose support has been immense and unwavering

TABLE OF CONTENTS

	Page
LIST OF FIGURES	iv
ACKNOWLEDGMENTS	v
ABSTRACT OF THE THESIS	vi
INTRODUCTION & BACKGROUND	1
Photothermal Heating of Nanoparticles	3
Carbon Black Nanoparticles	4
Radical Polymerization of Vinyl Monomers	6
Decomposition of Benzoyl Peroxide to Initiate Radical Polymerization	7
Other Reactions Initiated by Photothermal Heating	9
EXPERIMENTS & RESULTS	11
Bulk Radical Polymerization Initiated by Benzoyl Peroxide	11
Characterization of Resulting Poly(Methyl Acrylate)	15
Kinetics of Benzoyl Peroxide Decomposition in Ethyl Acetate	18
CONCLUSION	22
REFERENCES	24

LIST OF FIGURES

		Page
Figure 1	Photothermally Heated Particle in Solution	2
Figure 2	Solar Emission and Carbon Black Absorbance Spectra	4
Figure 3	Radical Polymerization Reaction Scheme	6
Figure 4	Pictures of Experimental Setup and Poly(Methyl Acrylate)	11
Figure 5	Thermal Images of Autoacceleration Event	12
Figure 6	Example Thermal Traces for Polymerization Experiments	13
Figure 7	Autoacceleration Times for Polymerization Experiments	14
Figure 8	GPC, ¹ H NMR and MALDI-TOF Spectra for PMA Samples	15
Figure 9	DSC Traces for PMA Samples	17
Figure 10	SEM Images of Various PMA Samples	18
Figure 11	HPLC Trace of Ethyl Acetate/BPO Solution	19
Figure 12	BPO Kinetics Results	21

ACKNOWLEDGMENTS

First, I would like to express my deep gratitude to Dr. Rachel Steinhardt, my partner in this project and without whom this research would not have been possible. I also want to thank my advisor, Dr. Aaron Esser-Kahn for his guidance and support throughout this project and in my first few years of graduate study.

I would like to thank both of my committee members, Dr. Zuzanna Siwy and Dr. Shane Ardo for donating their time and energy.

Much of this research presented here along with the figures are also components of a paper co-authored by Dr. Steinhardt and myself, which is currently in submission.

Financial support for this research was provided by the Department of Defense by way of the Air Force Office of Scientific Research.

ABSTRACT OF THE THESIS

Photothermal Heating of Nanoparticles for Radical Polymerization

By

Timothy McCormick Steeves

Master of Science in Chemical and Materials Physics

University of California, Irvine, 2017

Associate Professor Aaron Esser-Kahn, Chair

We report that photothermal heating of nanoparticles in solution can be achieved via a superheated state of the particles. This state creates nanoscale reaction zones around the particles that reach reaction temperatures far above the bulk solution temperature. These heterogeneous reaction systems improve efficiency in heat driven reactions and the length scale of heating provides new reaction dynamics. To test if these reaction conditions were amenable to traditional organic reactions, we tested if photothermal heating of nanoparticles initiated a radical polymerization. Radical-initiated polymerization of acrylates is a well-studied process initiated heating molecules that decompose into radicals. These radicals, in turn, go on to begin the polymerization process. We report a method where radical polymerization is initiated via photothermal heating of carbon black nanoparticles using a solar simulator. These polymerizations proceed five times faster than polymerizations held at the same measured bulk temperature. Additionally, uniform fibrous morphologies appear at the micron scale when the polymer is examined via SEM. Finally, we report that the photothermal heating acceleration of benzoyl peroxide decomposition results in an order of magnitude increase in reaction rate over bulk heating.

INTRODUCTION & BACKGROUND

Chemical reactions done in the laboratory or in a factory tend to be done with homogeneous mixtures or in simple binary systems, where two liquid phases are combined, or a solid catalyst is added to a mixture. The theater of reaction is the mixture itself, or the interface between two phases, or the surface of the solid catalyst. Much of the time this is done for simplicity and in the laboratory control over experimental parameters. However, photothermal heating nanoparticles introduces another dimensionality of reaction space. The nanoscale heated surface and small volume around each particle is a new space in which to do chemical reactions. The way in which these nanoscale volumes of heat interact with chemical reactants and the bulk solution provides new opportunities for chemical reactions by allowing for finer control over the amount of reactant heated and the time at which it is heated. In these experiments, we probed this new reaction space by using nanoscale heating to decompose benzoyl peroxide for radical vinyl polymerization.

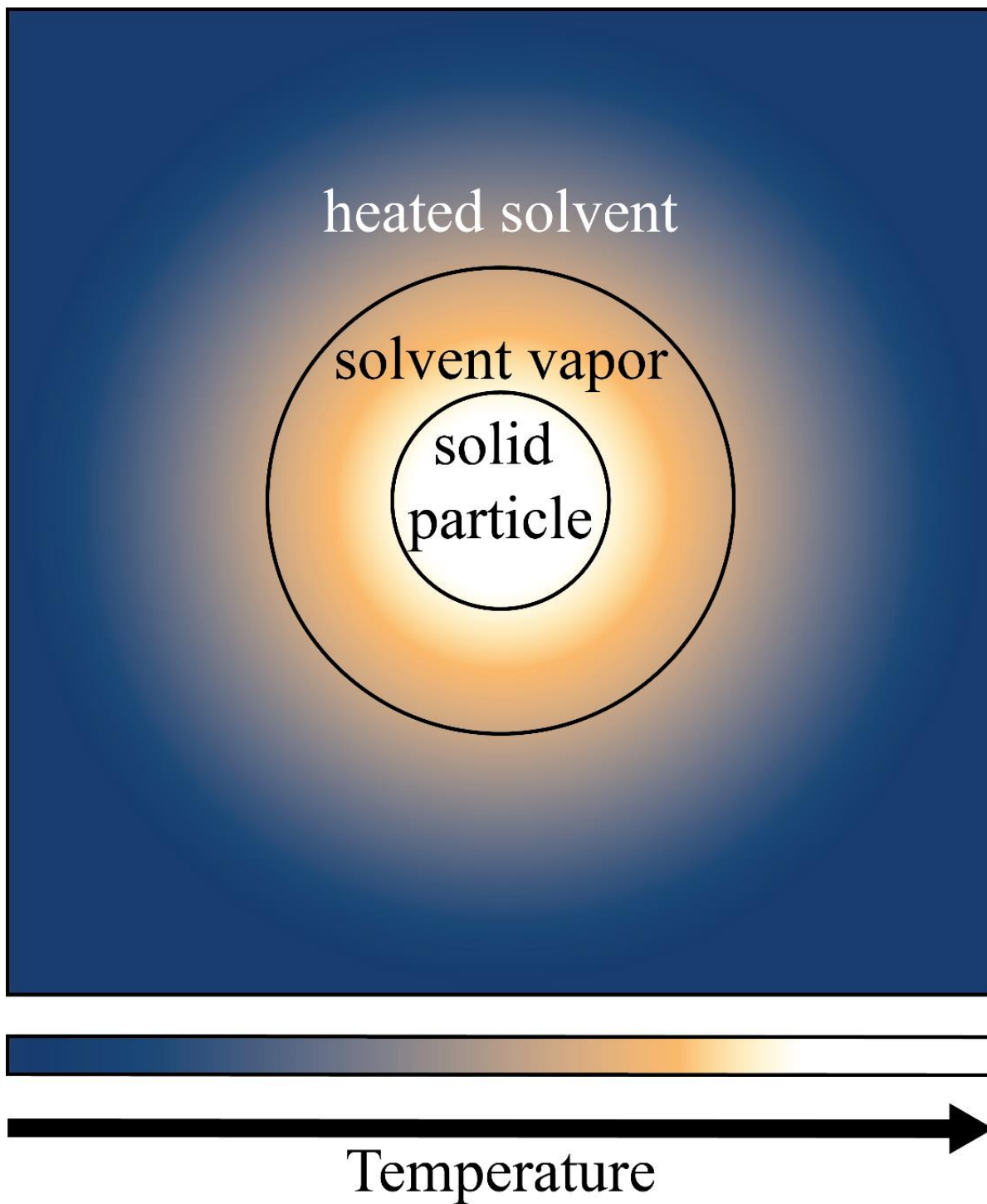


Figure 1. A photothermally heated nanoparticle in solution, heated to the point where it has vaporized a small amount of solvent around it, further insulating the particle from the surrounding solution. The volume of vapor around it, the surface of the particle itself, as well as a certain volume of liquid around the vapor bubble are all heated well above the bulk temperature, and may therefore be the location of profoundly different reactivity than the bulk solution.

Photothermal Heating of Nanoparticles

Photothermal heating is a well-studied process by which light is converted to heat by absorption of photons, on the nanoscale or in bulk materials.¹ Light absorption promotes an electron in the nanoparticle to a higher-energy vacant orbital which then transitions to a vibrational state, which means that energy has now been successfully converted from light to heat². (If metal nanoparticles are used and the light source is a laser at the on-resonance wavelength of the plasmon this results in very high light-to-heat conversion³.) Nanoparticles have very little mass, and a significantly lowered ability to conduct heat away from them compared to macroscopic versions of the same objects. In models for metal nanoparticles, heat is distributed throughout the nanoparticle evenly, and then the surface of the particle heats a small radius surrounding the particle, with the temperature falling off proportional to $1/r$ where r is the distance from the center of the particle². The result is particles that reach a superheated non-equilibrium, where they are much hotter than the bulk solution temperature, in many cases extending beyond the boiling temperature, which can create a small vapor-based shell that further insulates the particle. This is shown visually in Figure 1². This nanoscale heating phenomenon has been used as an effective solution or augmentation to numerous problems and processes, including steam generation, desalination, release of CO₂ from a capture solution, and heat-based tumor destruction⁴⁻⁷.

For these experiments, we've used carbon black nanoparticles. Instead of utilizing plasmon resonance, carbon black is a substance with very high absorbance across the solar spectrum, including visible light along with much of the ultraviolet and infrared spectrum⁸. This broad absorbance makes the sun the ideal candidate for an energy source. In contrast, plasmonic heating of metal nanoparticles can be very effective in its specific temporal and energetic

control, but requires light at a very particular wavelength to maximize the heating effect and is much more expensive due to both the costs of the metal nanoparticles and the cost of a laser. Carbon black is cheap and safer to work with than many metal nanoparticles, making it attractive for its simplicity as well as its effectiveness.

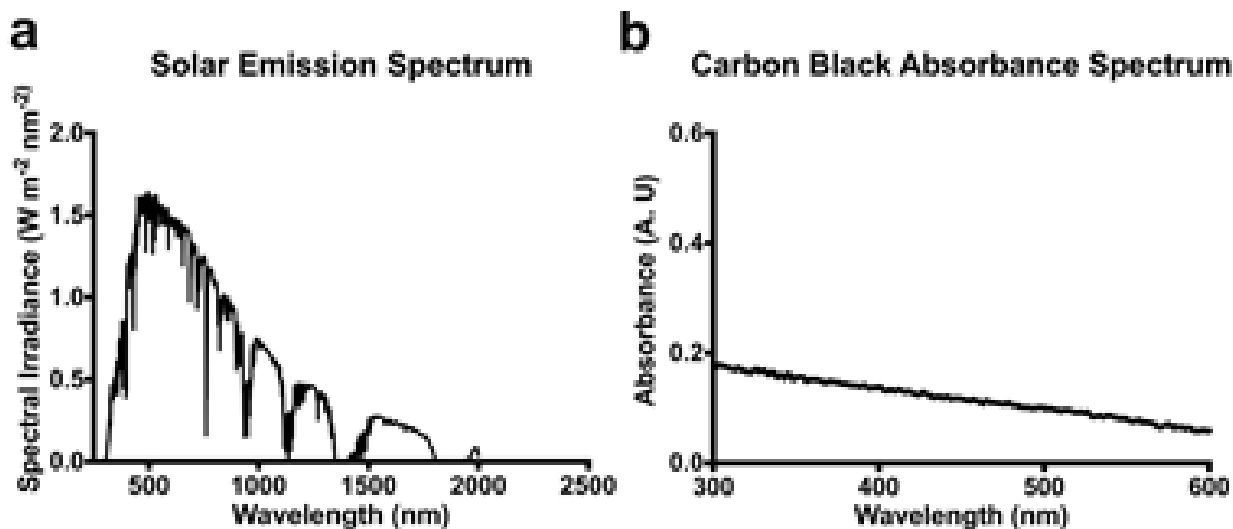


Figure 2. Comparison of a) solar emission spectrum (NIST) and b) carbon black absorbance spectrum, intended to highlight the strong coverage of carbon black for the entire spectrum.

Carbon Black Nanoparticles

Carbon black is a cheap versatile material commonly used as a rubber and paint additive⁹. It's formed through many different, though chemically similar, pathways consisting of incomplete combustion or decomposition of various hydrocarbons¹⁰. It is similar in composition to soot, but with a more careful synthesis that results in significantly greater carbon content than soot¹¹. The particle used in these experiments is a furnace black, made by injecting liquid fuel into the flame of a combusting gas. The resulting soot-like solid is separated and pulverized to create the product. As a choice for photothermal polymerization, carbon black particles are an ideal choice, as they are already widely used due to their ability to absorb as much light as possible without taking up a significant volume of the solution. Dispersions used in this experiment are visibly opaque with only a 1 mg/mL formulation. With any photothermal heating

solution, the goal is for the solution to be opaque (so no light escapes the solution) without being so concentrated that all of the light is absorbed near the surface of the flask. Carbon black's effective absorption of a wide spectrum of light allows it to rapidly superheat and initiate the reaction. Carbon black particles may also enhance this process due to their ability to chemisorb and stabilize free radicals¹⁰. This was a property only identified recently in our research, and it may be worthwhile to compare carbon black's effectiveness with another photothermally heated nanoparticle.

As an additive, carbon black adds color, increases heat and electrical conduction, protects the rest of the material from light, and also acts as a filler, reducing the amount of polymer needed for a given amount of polymer product⁹. It is present in many plastics and rubbers along with dyes and pigments for paints and inks. The results of this study are therefore immediately applicable to the production of a polymer product. The morphological anomalies are also of interest as it relates to carbon black, since they seem to be an critical element of whatever unknown process creates the fibrous microstructure.

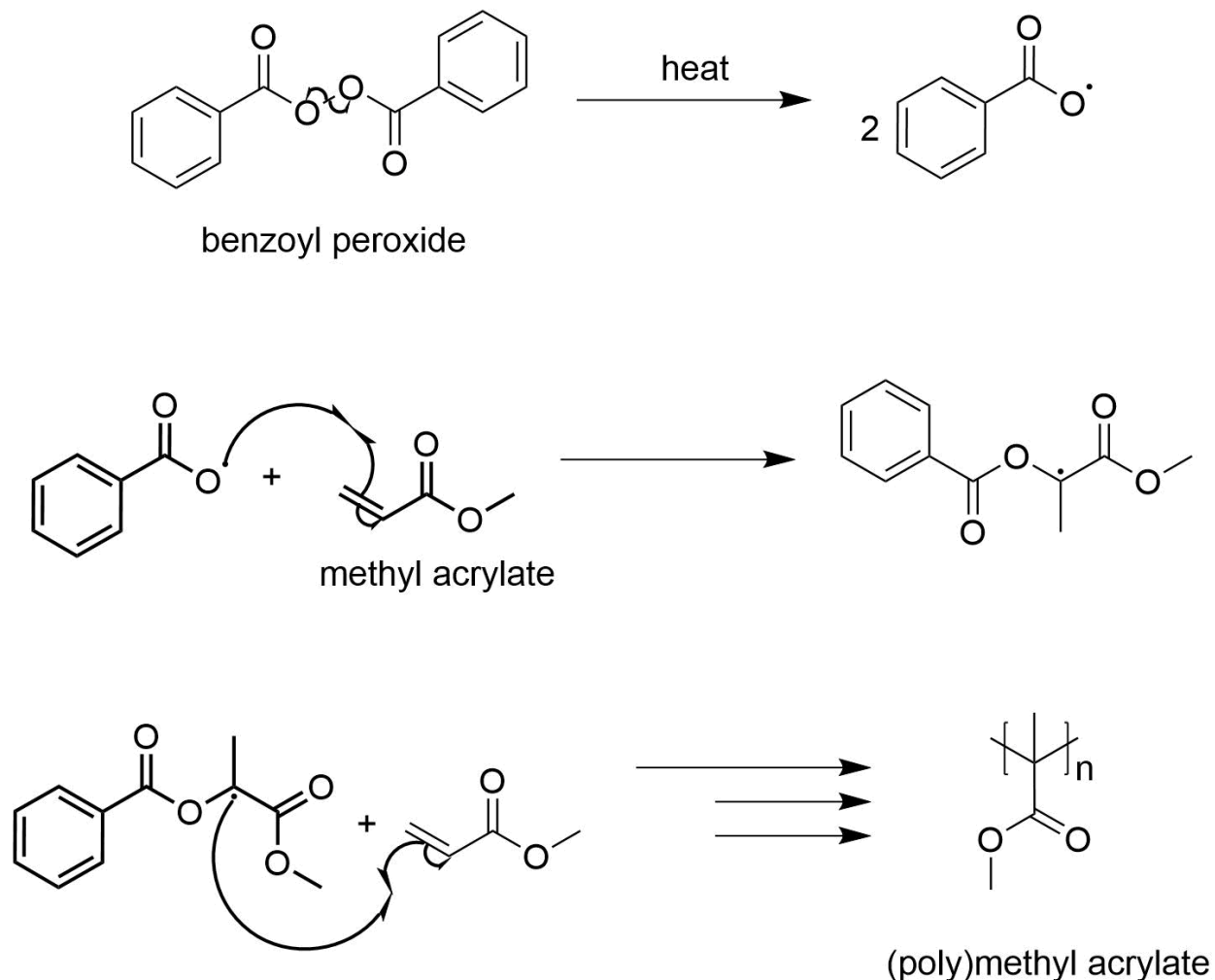


Figure 3. Schemes depicting the basic process for the free radical polymerization of methyl acrylate. In the first step the initiator, benzoyl peroxide, decomposes into two peroxy radicals which then go on in the following step to react with monomers to create actively growing chains. The final step encompasses the rapid growth and termination steps which the growing chains perform to form the final product polymer chains.

Radical Polymerization of Vinyl Monomers

Radical polymerization is driven by the action of radicals on various reactive vinyl groups. The basic reaction scheme for radical polymerization is shown in Figure 3. A radical is introduced into a solution which contains a monomer with a reactive vinyl group¹². The radical combines with one of the vinyl electrons to form a bond and a new radical located on the monomer¹². This process repeats with the new radical and another monomer until the chain is terminated by reaction with another radical in solution, either another growing chain or a

different free radical from the initiator¹². The process can be performed in a solvent, as an emulsion-based polymerization, or as a bulk polymerization with no solvent, the latter of which was used in this investigation¹². Radicals can be generated numerous different ways. Commonly they are generated from either heat-based or light-based decomposition of an initiator¹². In our experimentation, we focused exclusively on the thermal initiator benzoyl peroxide as our radical source.

Common monomers for radical polymerization are styrene, acrylates and methacrylates. These monomers polymerize to form polystyrene and acrylic, common polymers seen by the consumer in the form of packaging or insulation (for polystyrene) or any number of bendable hard plastics poly(methacrylates). The monomer most studied in this investigation is methyl acrylate, which is used in the production acrylic fibers and as an additive with other acrylic monomers.

Decomposition of Benzoyl Peroxide to Initiate Radical Polymerization

Core Process

The actual reaction being initiated by the heat is the decomposition of benzoyl peroxide into two separate peroxy radicals¹³. The bond between the two oxygens in the peroxide cleaves spontaneously and symmetrically when the temperature is high enough¹³. The symmetry of the cleavage is called homolytic, and results in one electron each from the broken bond staying on either side, forming two radicals. This reaction is the key in two of our experiments, first as a way to initiate radical polymerization in a bulk monomer solution via nanoscale heating of carbon black nanoparticles and then on its own within a solution of ethyl acetate to examine nanoscale heating's effects on the reaction kinetics. Benzoyl peroxide was an ideal target for the nanoscale heating because of its well-studied kinetics and high decomposition temperature.

Thermal decomposition of benzoyl peroxide doesn't occur significantly at room temperature and occurs at slow, manageable rate even at 56 °C, the highest temperature we observed in our illuminated carbon black solutions¹⁴. It is important to mention and highlight that although many radical initiators may be decomposed via visible light, benzoyl peroxide is specifically a thermal initiator, and is not sensitive to visible light.

Initiation of Radical Polymerization and Autoacceleration

As previously mentioned, once the peroxy radicals are formed in solution, they initiate polymerization. This polymerization occurs as chain growth, a process where chains extend rapidly and terminate much more quickly than they are generated, resulting in a reaction solution that is primarily monomer and completed polymer chains at any given moment¹². As the reaction continues and the composition of solutions becomes more viscous, the chains terminate less rapidly, as the active radical ends of the chains are immobilized by the viscous solution and are therefore unable to react with other chain ends, but are able to react with more monomer¹². This phenomena results in near-instantaneous completion of the reaction, as numerous immobilized growing chains rapidly consume all of the monomer present. An additional feedback loop is present in the form of heat from the exothermic reaction of chain growth. This heat rapidly increases the temperature of the solution, and this in turn increases the rate of the reaction. It can also melt vessels and boil the solution, so caution must be observed and autoacceleration is often viewed as a dangerous or destructive phenomenon. However, for our purposes, it serves as a highly useful endpoint metric. Autoacceleration occurs at a certain degree of conversion each time, and puts out enough heat that it's simple to measure. The time it takes the reaction to reach the autoacceleration point is a measure of the generation rate of the radicals.

Other Reactions Initiated by Photothermal Heating

Photothermal heating of nanoparticles activates reactions by way of highly localized heat. In our system, it's important to distinguish this activation from the activation due to bulk heating that occurs as a side effect of this nanoscale heating. We do this through controls, but there are several other examples in the literature that are able to work around this issue in other ways. The Lear lab utilized plasmonically heated gold nanoparticles to crosslink polyurethane in a solution¹⁵. They were able to precisely control the amount of light entering the system by using a pulsed laser light source and compare it to the baseline room temperature reaction. Since the laser pulses didn't measurably heat the bulk solution, any increase in reaction rate was due solely to the photothermal heating of the nanoparticles. They observed a billion-fold increase in reaction rate during the laser pulses. They chose to examine a reaction system where bulk heating was precluded due to the weak nature of the bond being formed, as it would break the bond attempting to be formed. So despite the fact that the reaction volume around the particles was hot enough that it would be completely unsuitable for a bulk reaction, the scale of the system allowed for the reaction to occur effectively within that heated volume, and with a profound increase in the rate of the reaction. This highlights the benefit that nanoscale heating can introduce to chemical synthesis. Both the localization and the timescale work in favor of this reaction.

In the Linic lab, they've examined silver metal nanostructures that can be used as catalysts for several reactions, including ethylene epoxidation. These systems were able to quadruple their reaction rate simply by illuminating them with a visible light spectrum illumination source¹⁶. They've also probed the mechanism of charge transfer between metal nanoparticles that are illuminated and have molecules bound to the surface¹⁶.

In the Esser-Kahn lab, we've used carbon black to release carbon dioxide from capture solutions. In these reactions, the target product is a gas, and since it releases when the solution is heated, the particles are rapidly surrounded by the gas product, and buoyed to the surface to release it⁶. In Figure 1, the bubble is labeled as vaporized solvent, but when the product of a reaction favored at higher temperatures is a gas, it can also be product. The result is a system that releases CO₂ at a much higher rate than the bulk temperature of the solution would generally allow for⁶. This is another example of the nanoscale heat localization working in favor of the reaction.

EXPERIMENTS & RESULTS

Bulk Radical Polymerization Initiated by Benzoyl Peroxide

In this experiment photothermal heating is compared with traditional bulk heating as a method to decompose benzoyl peroxide and initiate radical polymerization. Solutions of monomer and initiator are prepared with carbon black nanoparticles dispersed. The solutions are illuminated and their temperature is monitored over the course of the reaction. The thermal control is created by placing the same solutions in an oil bath held at the same temperature as that the photothermal solutions reach before autoacceleration occurs. The autoacceleration of the bulk polymerization is chosen as the endpoint with the peak of the exotherm marked as the time at which the reaction is completed. Methyl acrylate was the primary monomer of interest, but both methyl methacrylate and ethyl acrylate were also tested.

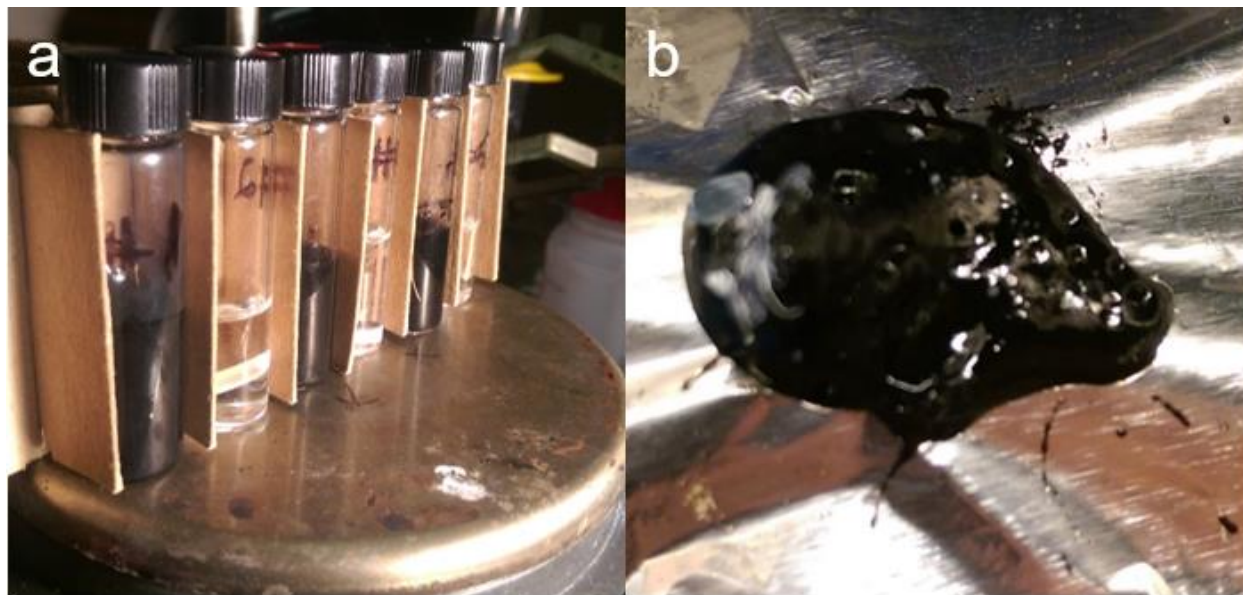


Figure 4. Pictures of a) preliminary experimental setup for photothermal polymerization and b) poly(methyl acrylate) product polymer that bubbled out of the solution vial after autoacceleration.

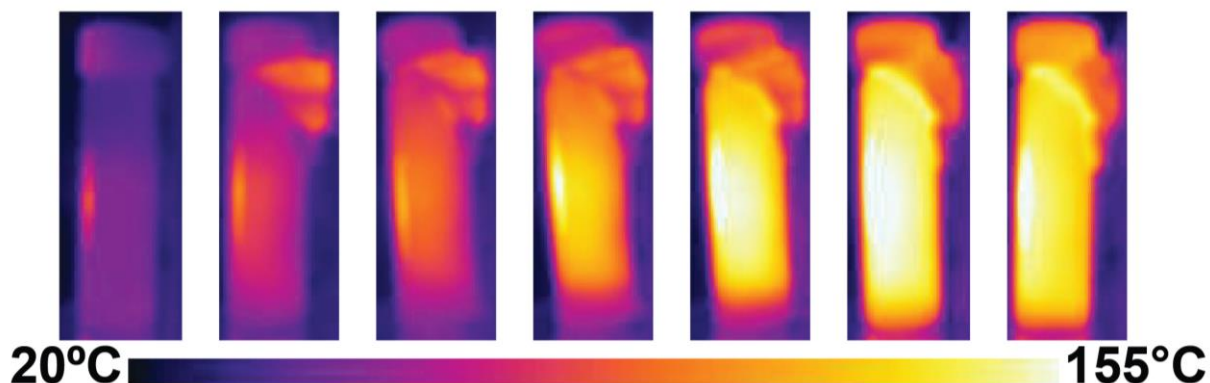


Figure 5. Thermal images taken by a Forward Looking Infrared (FLIR) camera depicting the autoacceleration point of these experiments. In the first image the solution is stirring at a stable temperature while being illuminated. Once autoacceleration begins heat rapidly evolves and the solution solidifies into a solid mass of polymer while giving off an immense amount of heat. Some polymer escapes the flask through the cap due to pressure. Pictures all taken over the course of a few seconds.

Experimental Details

4 mL monomer solutions are prepared with 4 mg/mL benzoyl peroxide and 1 mg/mL carbon black nanoparticles, along with a small stirbar. Benzoyl peroxide concentrations were chosen based on comparable values used in literature for similar polymerizations and carbon black concentrations were chosen based on previous work performed in the Esser-Kahn lab. Controls are run without carbon black, without benzoyl peroxide, and without both, The solutions that contain only benzoyl peroxide react, though much later than the test mixture. Solutions are capped and sonicated in a bath for 16 minutes to disperse particles. Vials are placed on a stir plate in a custom fabricated holder and stirred while thermocouples are placed into the solutions. For methyl methacrylate, the system is placed in inert atmosphere. Thermocouples record the temperature while the light source is turned on and the reaction is monitored. This light source is a solar simulator and has an irradiance of 1700 W/m^2 , approximately three times the intensity of the sun. The reaction is monitored and eventually reaches the autoacceleration point, and the vial heats rapidly and violently, giving off steam as the polymer instantly solidifies

(Figure 5). The peak of the thermal trace is recorded as the endpoint of the reaction. The thermal trials for methyl and butyl acrylate take the base bulk temperature recorded on the thermocouple in the light trials (56° C) and hold the reaction flask at this temperature to give a point of comparison. For methyl methacrylate, instead of a thermal trial, the no carbon black control was used, as this also polymerized after a certain time. In Figure 4, several characteristic thermal traces are displayed for both types of trials, the autoacceleration point is very obvious in both the light based trials and the thermal controls.

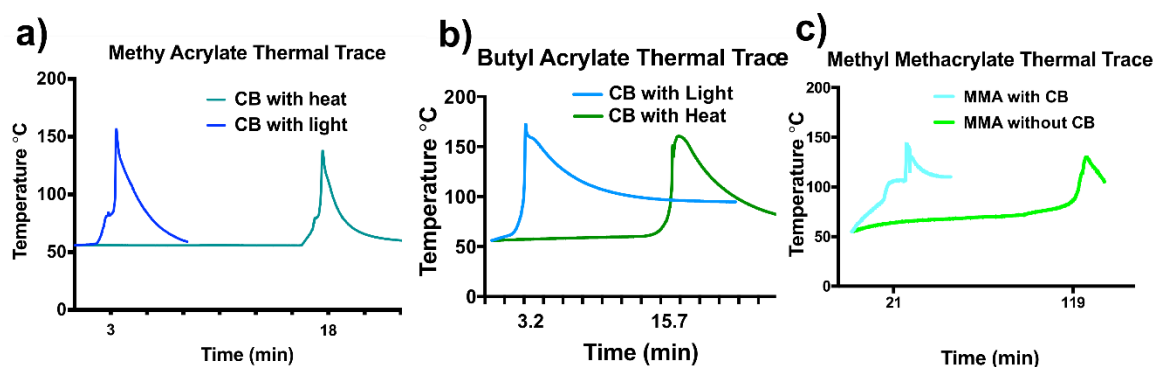


Figure 6. Characteristic thermal traces of reactions comparing the reactions that are treated by illumination and the reactions that are heated. For all three monomers the light based system reaches its autoacceleration point well before the oil bath heated trials.

Results

For all three tested monomers, the time to exotherm was consistently much lower for trials that were illuminated rather than heated in an oil bath. For both, the time to exotherm was less than five minutes, while for the thermal trials the time to exotherm was more than three times as long. A similar trend held for the methyl methacrylate trials, although in this case both polymerization took significantly longer to reach an endpoint (21 and 119 minutes). These results indicate that the polymer growth occurs significantly faster in the photothermally heated reaction, despite the fact that both reaction mixture's bulk temperature is identical. The fact that this works across multiple different monomer systems indicates that this enhancement is not

related to the monomer used but rather to the enhancement of initiator decomposition as previously hypothesized.

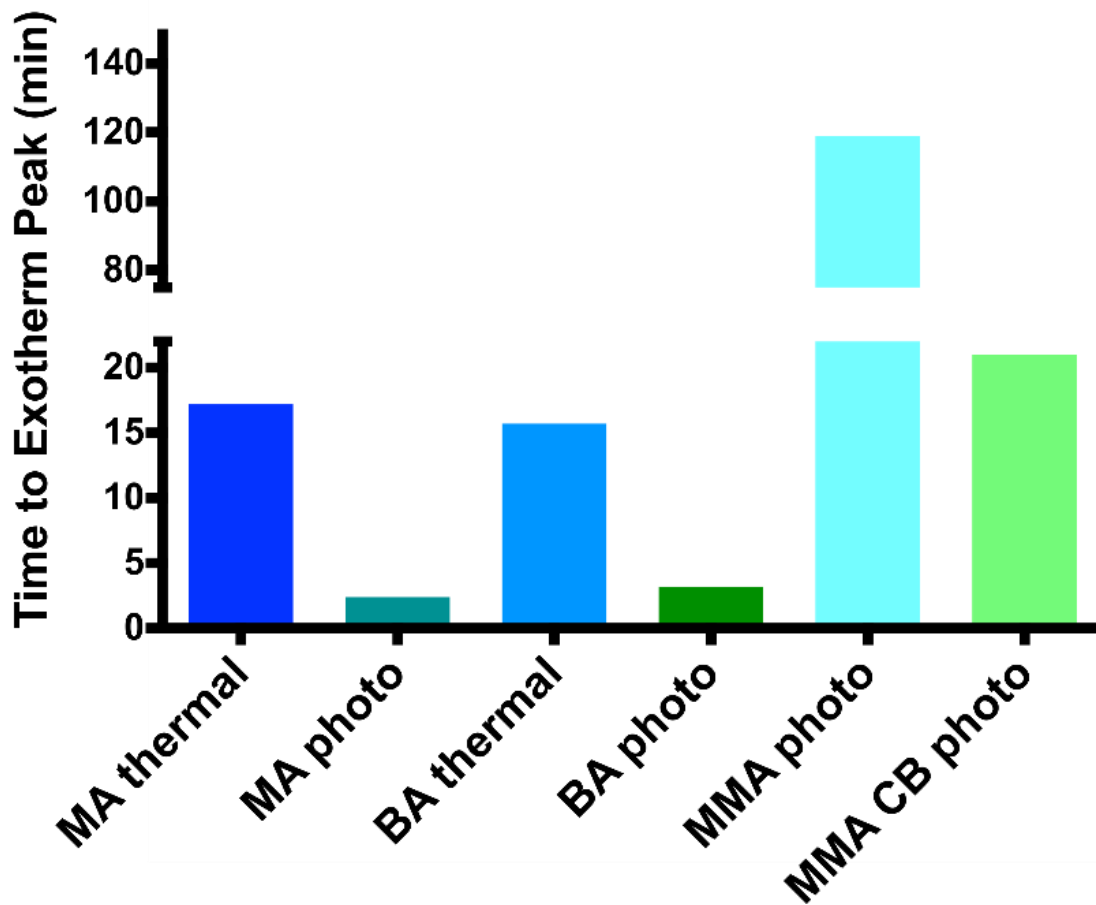


Figure 7. Bar graph depicts endpoints for various radical polymerization conditions. photo: photothermally initiated; thermal: thermally initiated via bulk heating; MA: methyl acrylate; BA: butyl acrylate; MMA: methyl methacrylate

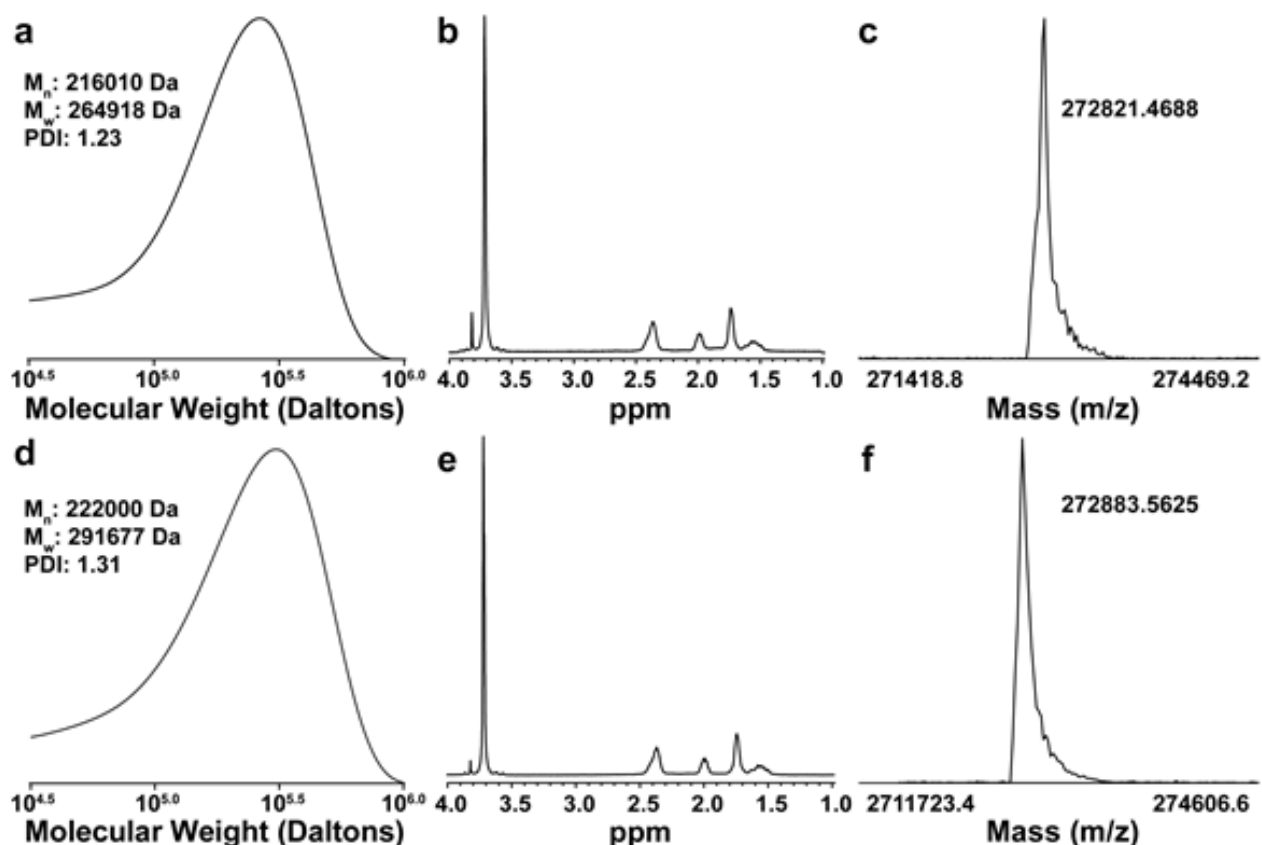


Figure 8. Graphs showing the results of analytical tests on photothermally initiated (top row) and thermally initiated (bottom row) poly(methyl acrylate). a) GPC trace of photothermally initiated methyl acrylate b) ^1H NMR of photothermally initiated methyl acrylate c) MALDI mass spectrum of photothermally initiated poly(methyl acrylate) d) GPC trace of thermally initiated methyl acrylate e) ^1H NMR of thermally initiated methyl acrylate f) MALDI spectrum of thermally initiated poly(methyl acrylate)

Characterization of Resulting Poly(Methyl Acrylate)

Molecular Weight Distribution

The resulting poly(methyl acrylate) polymer from both the thermal and photothermal trials was analyzed by GPC (gel phase chromatography), ^1H NMR (nuclear magnetic resonance) spectroscopy and MALDI-TOF (matrix assisted laser desorption/ionization – time-of-flight) mass spectroscopy, all of which are depicted above in Figure 8. The GPC peaks were calibrated using a polystyrene standard curve. The proton NMR was used for end group analysis to evaluate tacticity. All three tests indicated that the differently formed polymers were molecularly very similar. GPC shows very similar molecular weights and PDI measurements. The end group

integrations on the NMR are the same, indicating the same tactic properties. Visual inspection of the two spectra serve as a qualitative evaluation, as both the peaks and their relative ratios appear identical. And the MALDI shows very close agreement again with the molecular weight between the two samples. MALDI should give absolute molecular weights, whereas GPC compares to a standard curve, which may account for the discrepancy between the two measurements. The results of all three techniques indicate that the unique reaction process of photothermally initiated polymerization does not affect the core polymerization process involved and the resultant polymer is molecularly identical to the polymer formed through standard bulk heating-based initiation.

Glass Transition Temperatures

The resultant poly(methyl acrylate) of both the thermal control polymerization and the photothermally initiated polymerization were analyzed via Differential Scanning Calorimetry (DSC) to identify their glass transition temperature. They were taken through several cycles of heating and cooling before measurements to erase thermal history. After analyzing the traces in Figure 9, the resulting glass transition temperatures were determined to be 9.4 °C for thermally initiated poly(methyl acrylate) and 15.7 °C for photothermally initiated poly(methyl acrylate). This increase in glass transition temperature for the photothermally initiated polymer is small but significant. These results, when taken together with the information about the molecular similarities of the two polymers suggest that differences may exist on the nano or micro scale of the polymer which affect its ability to reorganize into an amorphous state.

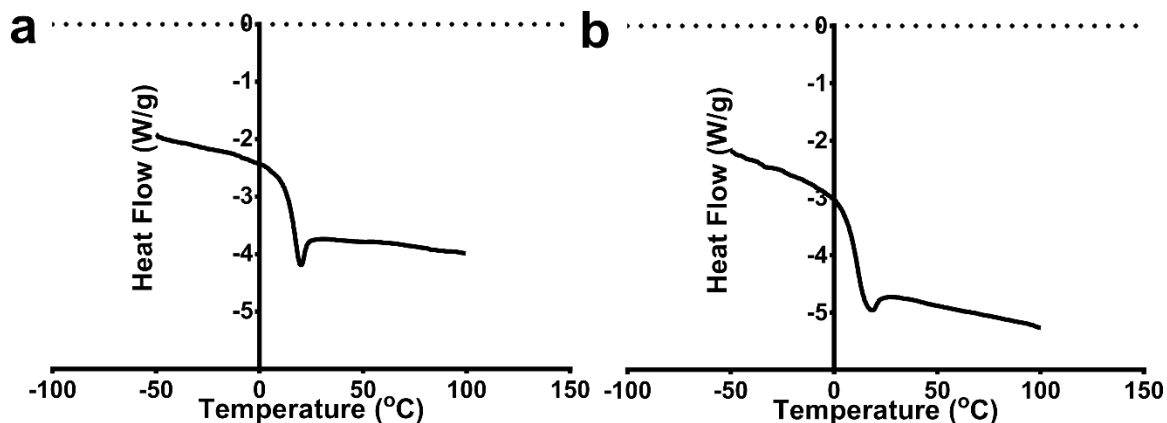


Figure 9. DSC traces of a) photothermally initiated poly(methyl acrylate) and b) thermally initiated poly(methyl acrylate)

Morphological Differences

Perhaps most interesting is the morphological differences visible in scanning electron microscopy (SEM) images of the polymers. The photothermally initiated polymer consistently had a uniform and ordered fibrous pattern. The top row of images in Figure 10 all depict this phenomenon. The fibers are directionally aligned, uniform and consistent in their radii ($1.16 \mu\text{m} \pm 0.04 \mu\text{m}$). This morphological variation did not replicate for other polymers such as butyl acrylate or methyl methacrylate or for the standard thermal polymerization of methyl acrylate (shown in Figure 10-e).

Based on the data above this morphological artifact is specific to both the monomer, methyl acrylate, and the polymerization method of utilizing photothermal heating with carbon black nanoparticles. Different concentrations of carbon black were also examined, to identify the threshold required for the “nanofibers” to develop and to see if the morphological order varied with carbon black concentration. It was identified that that fibers appear with carbon black concentrations as low as 0.25 mg/mL. When the concentration is increased from 5 mg/mL in the standard experiments to 20 mg/mL or 50 mg/mL as in images e) and f) in Figure 10, the fibrous structure is present but more chaotic and has a three dimensional organization.

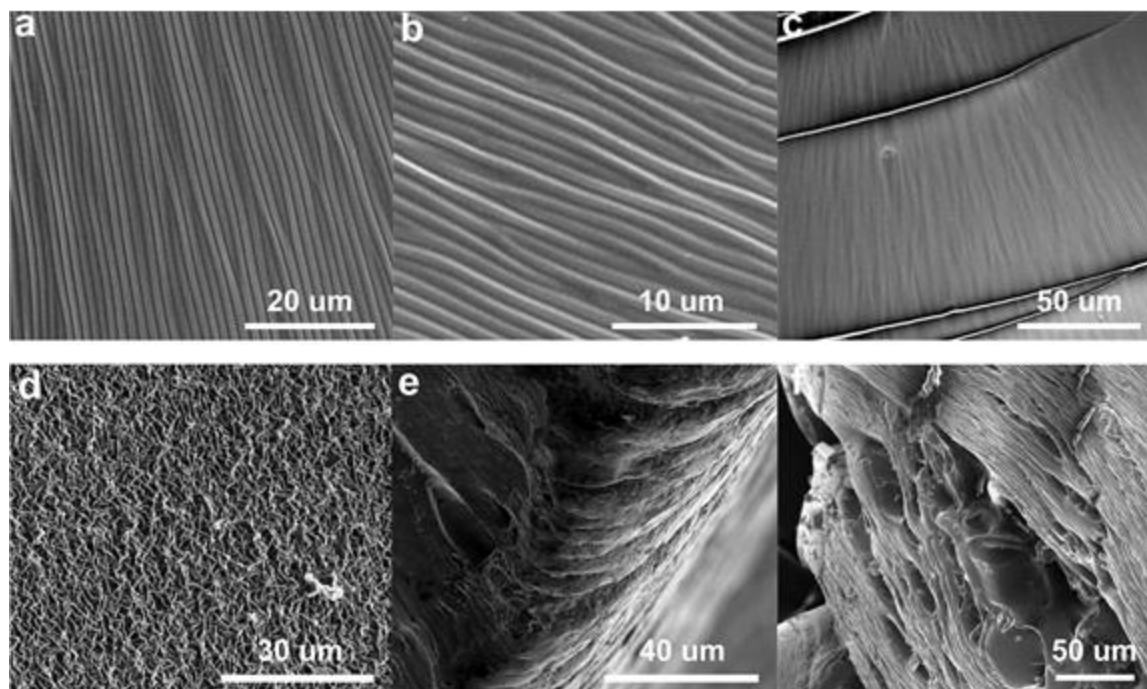


Figure 10. SEM of photothermally- and thermally-initiated polymers. (a) photothermally-initiated MA polymer at 2499 \times magnification; (b) photothermally-initiated MA polymer at 5000 \times magnification; (c) photothermally-initiated MA polymer at 850 \times magnification; (d) thermally-initiated polymerization at 2000 \times magnification; (e) lamellae of photothermally-initiated polymer with 50 mg/mL carbon black loading, 1500 \times magnification; (f) lamellae of photothermally-initiated polymer with 20 mg/mL carbon black loading, 650 \times magnification. Panels (a)–(c) show samples taken from three separate polymerization reactions.

Kinetics of Benzoyl Peroxide Decomposition in Ethyl Acetate

In order to further probe the enhancement of benzoyl peroxide decomposition, carbon black was added to solutions of benzoyl peroxide in ethyl acetate. Then the samples were treated with light or heat as the previous polymerization experiments. The concentration of benzoyl peroxide was monitored directly by high-performance liquid chromatography (HPLC) and these data were analyzed to evaluate the kinetics of the process.

Experimental Details

Ethyl acetate solutions with concentrations of 1 mg/mL carbon black and 5 mg/mL benzoyl peroxide were sonicated and then either heated in a thermal bath or illuminated for a set period of time. This experiment was designed to mimic the polymerization procedure. At set

time points, solutions were removed from heat or illumination, then filtered and run on the HPLC to calculate benzoyl peroxide concentration. The peak at 24 minutes shown in Figure 11 below was used to analyze the benzoyl peroxide concentration. Standard solutions of benzoyl peroxide in ethyl acetate were used to create a standard curve based on peak area. Three replicates of nine different concentrations were used for the standard curve and then three separate trials were run for each of the photothermal and the thermal treatments with eight time points over the course of two hours.

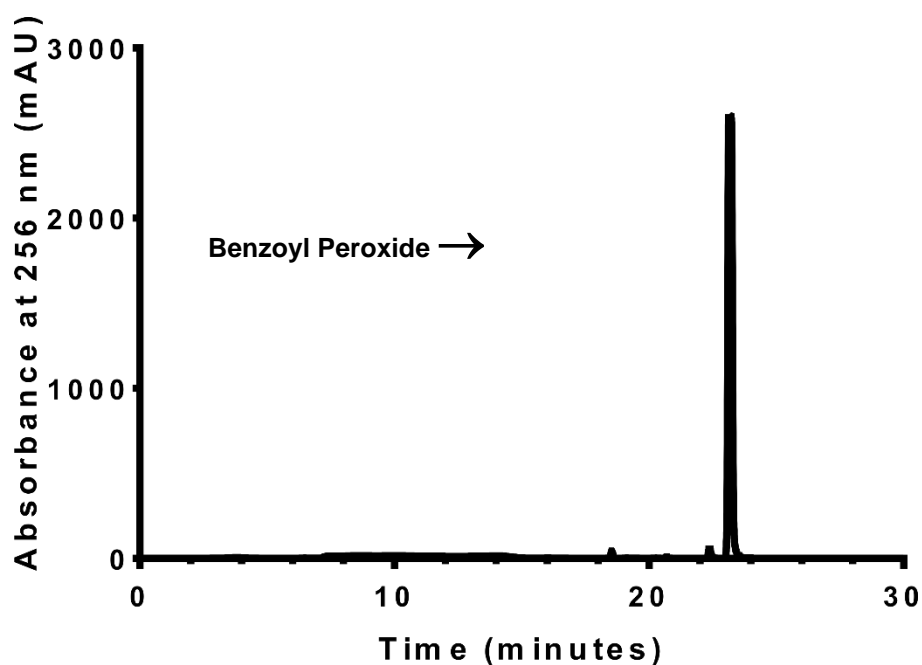


Figure 11. HPLC trace identifying the peak used to evaluate benzoyl peroxide concentration, the peak at 24 minutes was integrated and compared to a standard curve to determine benzoyl peroxide concentration

Results

The kinetics of photothermal heating are complex and difficult to analyze due to the unknown heat distribution within the reaction vessel. Currently we lack the ability to know enough of the spatial and temporal information relevant to the reaction to fully understand how nanoscale heating affects reactions. In particular, the concentration of benzoyl peroxide around the nanoparticles may be vastly different than in the bulk solution due to depletion from the decomposition reactions. Because of these limitations, we examined the reaction data with some assumptions about the observable kinetics that would allow us to understand and compare them to a system without nanoscale heating. Based on data for the benzoyl peroxide concentration over time we concluded that the kinetics of the photothermal reactions most closely followed a first-order mechanism. We assumed that the reaction geometry was static over the course of the experiment since the amount of carbon black, the rate of stirring and the bulk temperature were all held constant, and so the rate should only depend on the concentration of benzoyl peroxide. The thermal control allows us to compare our photothermal system to a system that is only reacting due to bulk heat, so any increase in the reaction rate should be attributable to the nanoscale heating from the carbon black particles. The result is a pseudo-first-order rate constant (summarized in Figure 12 b) that is an order-of-magnitude greater for photothermal heating compared to thermal heating. This confirms our earlier results indicating that photothermal heating increased the rate of reaction of the system without increasing the overall bulk temperature.

The kinetics of the reaction were analyzed assuming a first-order mechanism, but the decomposition of benzoyl peroxide is only first order at infinite dilution due to competing decomposition processes¹³. This likely accounts for the lower values for the coefficient of

determination for the data from the thermal trials. In comparison to the thermal trials, the photothermal trials more closely follow first-order kinetics suggesting that this reaction geometry is able to avoid the competing processes that slow the reaction.

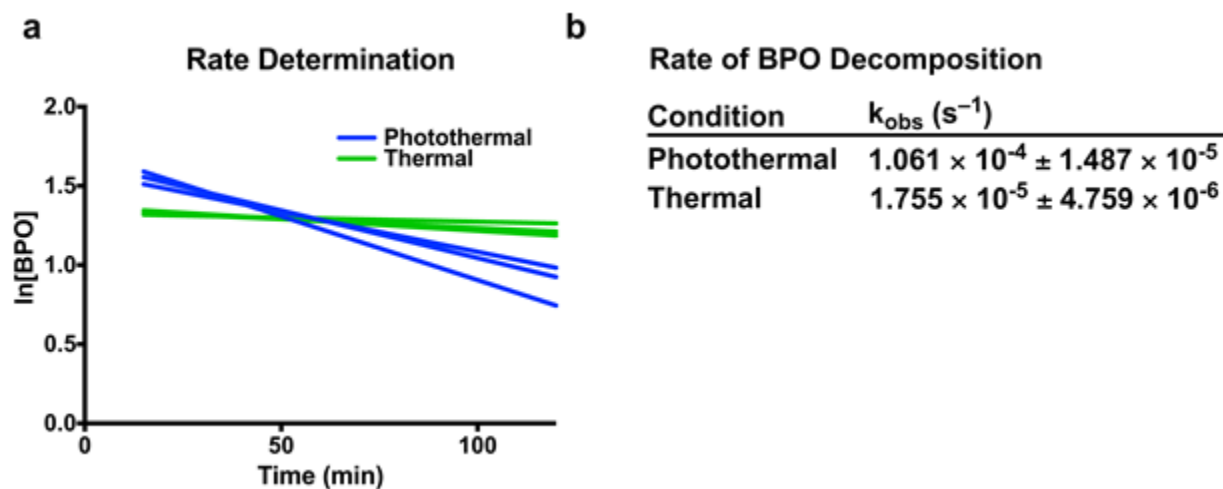


Figure 12. Graph depicting pseudo-first-order kinetics for both thermal and photothermal decomposition of benzoyl peroxide decomposition. a) shows the trendlines for the photothermal and thermal trials, the slope of these lines is the observed 1st order rate constant shown in b). The R^2 value for the photothermal lines ranged from 0.6316 to 0.7621 and from 0.1853 to 0.1066 for the thermal lines.

CONCLUSION

In this exploration of the power of photothermal heating to drive chemical reactions we've demonstrated that it can be used to enhance the rate of thermal decomposition for benzoyl peroxide. This enhanced reaction can then go on to drive radical polymerization of various vinyl monomers. The resulting poly(methyl acrylate) from these reactions exhibits unique morphological characteristics that suggest that the reaction geometry of nanoscale heating can introduce microstructured order to the resultant polymer in the form of fibrous structures.

The radical polymerization was activated via photothermal heating of carbon black nanoparticles. The polymerization was done neat, and the system was illuminated by a solar spectrum light set-up to deliver illumination at the level of three times the intensity of the sun as it reaches the earth's surface. The reaction rate was monitored by measuring the time it took to reach the autoacceleration point of the polymerization. The photothermal systems were able to reach this point approximately four times faster than an analogous system that was not illuminated but rather kept at the same bulk temperature as the photothermal system.

The resulting methyl acrylate polymers from the photothermal test reaction and the thermal control were analyzed by GPC, NMR and MALDI-TOF mass spectroscopy. The results indicated roughly the same molecular weight distribution and tacticity for the resultant polymers of both processes indicating that molecularly the product of both processes was essentially identical. However, these polymer samples were further analyzed for their glass transition temperature and imaged via SEM. The glass transitions for the photothermal polymer were inflated by 5 °C over the thermally initiated polymer and the SEM images of the photothermal polymer showed a fibrous morphology at the micron scale. Both of these indicate that the

nanoscale heating directs the polymerization to form a microstructured order that affects the properties of the resultant polymer.

Further investigation into this microstructured order is needed, as the mechanism by which nanoscale heating directs it will offer important information about how these particles operate in complex reaction environments.

Reaction kinetics of the benzoyl peroxide decomposition were examined in solutions of ethyl acetate, in order to examine this reaction separate from the radical polymerization and in order to be able to monitor the remaining benzoyl peroxide via HPLC. The results showed an order of magnitude increase in reaction rate for the photothermally heated reaction as compared to the reaction at the same bulk temperature, showing that nanoscale heating is responsible for the bulk of the benzoyl peroxide decomposition.

The benzoyl peroxide kinetics experiment and the polymerization experiment give two separate metrics showing the enhancement that photothermal heating has over bulk heating. This was the original objective of these experiments. Positive findings here direct us towards further exploration of other reactions that may be enhanced by the nanoscale heating of carbon black nanoparticles. I also think that exploring this reaction space from a computational perspective may give some insight into the exact mechanism of how this nanoscale heating affects reaction dynamics. Unexpected, is the morphological differences present in the poly(methyl acrylate) samples visible in the SEM images. Further probing may reveal unique information about how this dynamic system evolves over the course of the reaction. The fibers themselves may prove useful, and further exploration of their properties and manipulation is another possible extension of this research.

REFERENCES

- (1) Thomas, M. E. *Optical Propagation in Linear Media: Atmospheric Gases and Particles, Solid-State Components, and Water*; Johns Hopkins University/Applied Physics Laboratory series in science and engineering; Oxford University Press: Oxford ; New York, 2006.
- (2) Govorov, A. O.; Richardson, H. H. Generating Heat with Metal Nanoparticles. *Nano Today* **2007**, *2* (1), 30–38.
- (3) Eustis, S.; El-Sayed, M. Why Gold Nanoparticles Are More Precious than Pretty Gold: Noble Metal Surface Plasmon Resonance and Its Enhancement of the Radiative and Nonradiative Properties of Nanocrystals of Different Shapes. *Chemical Society Reviews* **2006**, *35* (3), 209–217.
- (4) Neumann, O.; Urban, A. S.; Day, J.; Lal, S.; Nordlander, P.; Halas, N. J. Solar Vapor Generation Enabled by Nanoparticles. *ACS Nano* **2013**, *7* (1), 42–49.
- (5) Dongare, P. D.; Alabastri, A.; Pedersen, S.; Zodrow, K. R.; Hogan, N. J.; Neumann, O.; Wu, J.; Wang, T.; Deshmukh, A.; Elimelech, M.; Li, Q.; Nordlander, P.; Halas, N. J. Nanophotonics-Enabled Solar Membrane Distillation for off-Grid Water Purification. *PNAS* **2017**, *114* (27), 6936–6941.
- (6) Nguyen, D. T.; Truong, R.; Lee, R.; Goetz, S. A.; Esser-Kahn, A. P. Photothermal Release of CO₂ from Capture Solutions Using Nanoparticles. *Energy Environ. Sci.* **2014**, *7* (8), 2603–2607.
- (7) Gobin, A. M.; Watkins, E. M.; Quevedo, E.; Colvin, V. L.; West, J. L. Near-Infrared-Resonant Gold/Gold Sulfide Nanoparticles as a Photothermal Cancer Therapeutic Agent. *Small* **2010**, *6* (6), 745–752.
- (8) Han, D.; Meng, Z.; Wu, D.; Zhang, C.; Zhu, H. Thermal Properties of Carbon Black Aqueous Nanofluids for Solar Absorption. *Nanoscale Res Lett* **2011**, *6* (1), 457.
- (9) Spahr, M. E.; Rathon, R. Carbon Black as a Polymer Filler. In *Polymers and Polymeric Composites: A Reference Series*; Palsule, S., Ed.; Springer Berlin Heidelberg, 2016; pp 1–31.
- (10) Donnet, J.-B.; Voet, A. *Carbon Black: Physics, Chemistry, and Elastomer Reinforcement*; M. Dekker: New York, 1976.
- (11) Watson, A. Y.; Valberg, P. A. Carbon Black and Soot: Two Different Substances. *AIHAJ* **2001**, *62* (2), 218–228.
- (12) Odian, G. G. *Principles of Polymerization*, 4th ed.; Wiley-Interscience: Hoboken, N.J, 2004.
- (13) Barnett, B.; Vaughan, W. E. The Decomposition of Benzoyl Peroxide. I. The Kinetics and Stoichiometry in Benzene. *J. Phys. Chem.* **1947**, *51* (4), 926–942.
- (14) Thermal Initiators: Decomposition Rate and Half-Life. Aldrich.
- (15) M. Haas, K.; J. Lear, B. Billion-Fold Rate Enhancement of Urethane Polymerization via the Photothermal Effect of Plasmonic Gold Nanoparticles. *Chemical Science* **2015**, *6* (11), 6462–6467.
- (16) Boerigter, C.; Aslam, U.; Linic, S. Mechanism of Charge Transfer from Plasmonic Nanostructures to Chemically Attached Materials. *ACS Nano* **2016**, *10* (6), 6108–6115.